Computational Prediction of Flow-Generated Sound

Meng Wang,[1] Jonathan B. Freund,[2] and Sanjiva K. Lele[3]

[1]Center for Turbulence Research, Stanford University/NASA Ames Research Center, Stanford, California 94305; email: wangm@stanford.edu

[2]Department of Theoretical and Applied Mechanics, University of Illinois at Urbana-Champaign, Urbana, Illinois 61801; email: jbfreund@uiuc.edu

[3]Departments of Mechanical Engineering and Aeronautics & Astronautics, Stanford University, Stanford, California 94305; email: lele@stanford.edu

Annu. Rev. Fluid Mech. 2006. 38:483–512

The *Annual Review of Fluid Mechanics* is online at fluid.annualreviews.org

doi: 10.1146/annurev.fluid.38.050304.092036

0066-4189/06/0115-0483$20.00

Key Words

aeroacoustics, flow noise, computational methods, acoustic analogy, turbulence simulation, noise control

Abstract

This article provides a critical review of computational techniques for flow-noise prediction and the underlying theories. Hybrid approaches, in which the turbulent noise source field is computed and/or modeled separately from the far-field calculation, are afforded particular attention. Numerical methods and modern flow simulation techniques are discussed in terms of their suitability and accuracy for flow-noise calculations. Other topics highlighted include some important formulation and computational issues in the application of aeroacoustic theories, generalized acoustic analogies with better accounts of flow-sound interaction, and recent computational investigations of noise-control strategies. The review ends with an analysis of major challenges and key areas for improvement in order to advance the state of the art of computational aeroacoustics.

1. INTRODUCTION

Flow-generated sound is a serious problem in many engineering applications. It can cause human discomfort and affect the stealth operations of military air vehicles and submarines. The most notorious flow noise is that from aircraft jet engines, which continues to be an area of intense investigations in response to tightening regulation of airport noise. In fact, the study of aeroacoustics, pioneered by Lighthill (1952), was prompted by the need for quieter jet engines. However, it is not hard to find other important noisy flows (Blake 1986). In naval applications, the noise generated by marine propellers, hydrofoils, and even transitional and turbulent boundary layers on sonar domes are serious concerns. It can not only affect the detectability of a submarine, but also interfere with the working of sonar devices if the self-noise signals cannot be distinguished from incoming acoustic signals. With advances in jet-noise reduction, fan noise from the turbo-fan engines rises in significance, and airframe noise, including the noise from the landing gear, slats, and flaps, becomes a significant component of overall noise, especially when landing. In the automotive industry, increasing attention is being paid to reducing wind noise, typically dominated by flows past sideview mirrors, A-pillars, and windshield wipers. Other examples include the noise from wind turbines, axial and centrifugal fans in rotating machines, and helicopter rotors.

Closely coupled with the computational prediction of sound is the designation of an effective noise source in the flow. There are many rational possibilities for viable sound sources (Ffowcs Williams 1977). In the first aeroacoustic theory by Lighthill (1952), sound is generated by unsteady flows through the nonlinear interaction of velocity fluctuations, entropy fluctuations, as well as viscous stress. Alternative but still exact formulations [e.g., Howe (1975), Powell (1964); see also the recent book by Howe (2003)] emphasize the role of vorticity as sound sources. In free space, where jet noise is usually considered, the dominant sources are relatively inefficient, becoming quadrupoles in the low-Mach-number limit. The presence of solid boundaries, as in the other examples mentioned above, generally makes the sound radiation more efficient. They can enhance noise radiation in two ways: by creating or augmenting noisy flow features such as unsteady separation and vortex shedding and by imposing a boundary inhomogeneity, which promotes efficient conversion of flow energy to acoustic energy.

The study of flow-induced noise, known as aeroacoustics or hydroacoustics depending on the fluid medium, is concerned with the sound generated by turbulent and/or unsteady vortical flows including the effects of any solid boundaries in the flow. The computation of these sound sources and sound propagation constitutes the main focus of the present review. Given the diverse and active nature of this field, it is not possible to provide a comprehensive review in this short article. The contents are highly selective, reflecting the authors' view of issues that are important. These include some formulation and computational issues in the application of aeroacoustic theories; emerging flow simulation tools for the nonlinear processes of sound generation; the development of general aeroacoustic theories, which have better accounting of flow-sound interaction; and applications of numerical prediction tools to

explore noise-control strategies. An extended version of this article is available (Wang et al. 2005). A number of recent review articles (Colonius & Lele 2004, Kurbatskii & Mankbadi 2004, Tam 2004, Wells & Renaut 1997) have focused more specifically on numerical aspects of computational aeroacoustics.

2. OVERVIEW OF COMPUTATIONAL AEROACOUSTICS

2.1. Computational Approaches

Computational techniques for flow-generated sound can be classified into two broad categories: direct computation and indirect, or hybrid, computation. The direct approach computes the sound together with its fluid dynamic source field by solving the compressible flow equations. Direct numerical simulation (DNS), which resolves all flow scales including the small dissipative scales, or large-eddy simulation (LES), which resolves only the dynamically important flow scales and models the effects of smaller scales, can be employed. It is also possible to use unsteady Reynolds-averaged Navier-Stokes (RANS) methods to compute the noise of the largest flow features. The simulation domain must be sufficiently large to include all the sound sources of interest and at least part of the acoustic near field. Extension to the acoustic far field can then be achieved using a variety of analytical and numerical means. Provided that a wave equation is satisfied at the edge of the simulation domain, an analytical solution to the wave equation using the Kirchhoff integral (Farassat & Myers 1988, Freund et al. 1996, Lyrintzis 2003) can be readily employed. Numerical means of solution extension typically involve solving simplified equations, such as the linearized Euler equations or wave equation, in a larger domain external to the domain of direct simulation (Freund et al. 2000).

Because it avoids any modeling approximations, the direct computation method using DNS provides a tool for studying sound-generation mechanisms and generating databases for developing and evaluating sound prediction models (Section 4.2). However, because of its high computational cost, its use is limited to simple flow configurations at low to moderate Reynolds numbers. The use of LES to expand this range of applicability remains an area of active research (see Section 4.3).

In a hybrid approach, the computation of flow is decoupled from the computation of sound, which can be done in a post-processing step based on an aeroacoustic theory (Section 3). The far-field sound is obtained by integral or numerical solutions of acoustic analogy equations using computed source field data. A fundamental assumption for acoustic analogy-based prediction is the one-way coupling of flow and sound, i.e., the unsteady flow generates sound and modifies its propagation, but the sound waves do not affect the flow in any significant way. Thus, the principal application of the hybrid approach lies in flows at low fluctuating Mach numbers. Time-accurate turbulence simulation tools such as DNS, LES, and unsteady RANS methods can be used to compute the space-time history of the flow field, from which acoustic source functions are extracted. At low Mach numbers, incompressible flow solutions can be adequate for approximating acoustic source terms (see Section 3.3). Because of the high computational cost of the time-accurate simulations, there have been efforts

to use steady RANS calculations in conjunction with a statistical model to generate acoustic source terms (Bailly et al. 1997, Khavaran & Bridges 2005). A hybrid approach is also attractive when only part of the sound can be computed directly. For example, in LES the smaller flow scales may be either absent or inaccurate. The sound of these "missing scales" can be "added" to the direct solution using acoustic theory.

2.2. Challenges and Simplifications

There are a number of distinct challenges posed by the computation of flow noise relative to general computational fluid dynamics, as anticipated early on by Crighton (1988) and recently discussed in detail by Colonius & Lele (2004). First, the noise-generating flow is inherently unsteady, which renders steady RANS methods alone unsuitable and unsteady RANS calculations generally insufficient except when the flow is dominated by simple large-scale oscillations. Modern turbulence simulation techniques such as DNS, LES, or integrated RANS/LES methods offer attractive alternatives, but they are not always affordable even with today's high-performance computers. The latter two of these approaches involve different levels of modeling and approximation whose effects on noise prediction have not been thoroughly examined.

The second difficulty is the vast disparity in the magnitudes of the fluid dynamic and acoustic disturbances. With the exception of high-speed flows involving shock waves, only a small fraction (~fourth power of fluctuating Mach number for small Mach number) of flow energy radiates to the far field (Crighton 1993). This places a stringent requirement on numerical accuracy if the sound and flow are to be computed simultaneously as in the direct method. In the hybrid approach, because the flow (source) and sound are computed separately, numerical accuracy for the flow simulation is less critical. Simpler, more flexible, but lower-resolution schemes are applicable provided that numerical dissipation is carefully controlled to prevent the artificial damping of high-frequency source components, and acoustic source formulations faithful to the true radiation characteristics (e.g., dipole, quadrupole, etc.) are used.

The scale separation between sound and flow is another salient feature of aeroacoustics, which can lead to both computational challenges and simplifications, depending on the method of choice. In an unconfined region, a sound wave matches the timescale of its fluid dynamic source, whereas its wavelength λ is related to the source (eddy) size ℓ by the fluctuating Mach number M: $\lambda = \ell/M$ (a Doppler factor should be added if there is mean flow). This creates a large length-scale disparity for low-Mach-number flows, making direct computation of sound difficult. On the other hand, a large scale-separation makes the use of hybrid methods ideal because the underlying assumptions are more easily justified. At the other extreme, if M is significantly greater than unity, scale separation and energy level disparity are diminished, but with the new complication of nonlinear acoustic propagation.

The case of high-subsonic-Mach-number flow, which is typical of jet engines in modern passenger aircraft, is particularly challenging due to the lack of clear scale

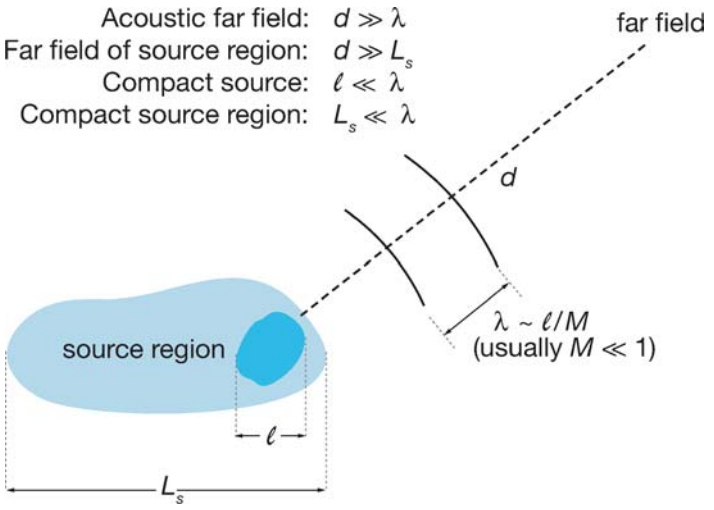

Figure 1

Schematic of source and sound scales.

separation. The flow and sound are difficult to separate in a meaningful way. In the application of acoustic analogies, this makes the designation of source terms versus propagation effects ambiguous at best, as discussed in Section 3.1.

This section closes by mentioning some frequently invoked approximations in aeroacoustics. Consider a source region of characteristic length scale L_s containing individual sources (eddies) of size ℓ (**Figure 1**). One simplifying concept is the acoustic far field, which is reached when the distance d to the closest point in the source region far exceeds the acoustic wavelength, i.e., $d/\lambda \gg 1$ or $d/\ell \gg M^{-1}$. In the integral forms of acoustic analogies, the use of leading-order terms in an acoustic far-field expansion (with respect to λ/d) leads to much simpler evaluations of sound. Further simplifications can be made if the observer location is also in the far field of the source region, i.e., $d/L_s \gg 1$. Another important concept is the compactness of acoustic sources (source regions). A source (source region) is considered acoustically compact if its extent is much smaller than the acoustic wavelength, or $\ell/\lambda \ll 1$ ($L_s/\lambda \ll 1$). In this limit, the source (source region) behaves as a simple point source, because the difference in times for sound signals emitted from various source locations to arrive at a given observation point (the retarded time difference) is negligible. This dramatically simplifies acoustic analogy-based computations. Given that $\lambda = \ell/M$, it is apparent that low-Mach-number flows are more likely to be acoustically compact. Even for a source region that is not acoustically compact overall, it may be compact in certain directions. In fact, based on elementary trigonometry, for an observer sufficiently far from a finite source region, the source planes perpendicular to the direction of propagation can always be made acoustically compact. This type of partial compactness can be exploited in the calculation of far-field sound to reduce the data storage requirement and simplify the solution process.

3. NOISE SOURCES AND HYBRID METHODS

3.1. Source versus Propagation

Definition of noise sources for use in computation or theory is inherently coupled to propagation effects, which simplistically refer to any alterations of the sound waves after they are generated. Dissipation can be considered a propagation effect, but typically propagation over many wavelengths is needed for significant dissipation, so this effect can be decoupled from the sound-generation mechanisms and treated independently. More important for flow-generated sound is refraction by sound speed and velocity gradients. This effect presumably neither increases nor decreases the energy carried by the waves, although defining acoustic energy in the presence of flow-acoustic interactions is complex.

From a modeling perspective, it makes certain intuitive sense to treat the different physical processes of sound generation and propagation as distinct: The first should create acoustic energy and the second alters its character. Although this picture is clear, implementation in a mathematical model for use in computational prediction or otherwise is less clear, and the picture is complicated further by the somewhat surprising result that flow, at least from a certain perspective, can alter the efficiency of an acoustic source (Dowling 1976, Goldstein 1975). In short, there are multiple viable ways to define sources and their corresponding propagation effects. The distinction is clearer in hydroacoustics, where small-Mach-number scalings more clearly delineate these effects, but these are unavailable for flows with $M \sim 1$. Mathematically, a flow solution $\mathbf{q}$, here written generically as a vector of velocities and thermodynamic variables sufficient to uniquely define a flow condition, satisfies the compressible flow equations: $\mathcal{N}(\mathbf{q}) = 0$. Part of $\mathbf{q}$ is sound, but without the benefits of scaling or other firm arguments its mathematical definition remains vague, except perhaps for weak disturbances (Chu & Kovásznay 1958). An acoustic analogy is formulated by rearranging $\mathcal{N}(\mathbf{q}) = 0$ into $L\mathbf{q} = S(\mathbf{q})$, where L is some (usually linear) wave propagation operator and $S(\mathbf{q})$ is then its corresponding nominal (nonlinear) sound source, which can be assumed to act analogously to an externally applied source, although in reality it is part of the same unsteady flow that locally makes up $L\mathbf{q}$. This decomposition, whatever motivates the particular form of L and S, is useful if L can somehow be inverted to provide $\mathbf{q}$ in the far field where it is acoustic.

The first and most well-known L–S decomposition is the Lighthill (1952) analogy:

$$\left(\frac{\partial^2}{\partial t^2} - c_0^2 \frac{\partial^2}{\partial x_i \partial x_i}\right)\rho = \frac{\partial^2 T_{ij}}{\partial x_i \partial x_j}, \qquad T_{ij} = \rho u_i u_j + p_{ij} - \delta_{ij} c_0^2 \rho. \tag{1}$$

In this case, L is a linear homogeneous-medium scalar wave operator acting on the density and thus contains no propagation effects. All the other terms representing different physics are lumped into S, defined as the double divergence of the Lighthill stress tensor T_{ij}, where p_{ij} is the stress tensor including pressure and viscous stress contributions. Because the Lighthill equation is exact, exact knowledge of S yields the sound via inversion of L, which is straightforward and is the basis of many prediction methods (Lilley 1996, Ribner 1969; see detailed discussions in Sections 3.2 and 3.3).

Mixing different physical mechanisms into S in Lighthill's theory has been thought to hamper modeling and prediction, which motivated acoustic analogies that more clearly make this distinction. Lilley (1974), for example, formulated an acoustic analogy in which L is the Pridmore-Brown (1958) operator (see also the discussion of Goldstein 1984), which is attractive because it explicitly models some of the refraction physics of a parallel shear flow. The Lilley equation also serves as the basis of several computational predictive strategies (Bailly et al. 1997, Khavaran & Bridges 2005). Colonius et al. (1997) undertook an extensive analysis of this based on DNS data. A conclusion of their work was that remarkable care was required in evaluating S to make accurate computational predictions of far-field sound. A further aspect of Lilley's $L\mathbf{q}$, which is challenging both for mathematical analysis and numerical inversion, is that it supports homogeneous instability wave solutions that grow exponentially in space. These issues provided some of the motivation for Goldstein (2003) to derive a generalized acoustic analogy, which serves as a rational theoretical basis for several classes of predictive computation. In his formulation, the selection of an arbitrary base flow, whose refractive and other propagation properties are incorporated into L, automatically sets S. In the spirit of Lighthill's original acoustic analogy strategy, the generality of this formulation allows most approximations to be made after the exact formulation is crafted, which should clarify their implications. Both the Lighthill and Lilley equations are representable within Goldstein's framework, as are acoustic analogies based on steady spreading or even time-dependent base flows. For a jet configuration, if only the steady transverse shear terms are retained in L, the propagation operator matches that used by Tam & Auriault (1999), although the source S that results is very different from their ad hoc selection. This should increase the domain of accurate predictions beyond where the ad hoc model is parameterized.

Ultimately, for use in a computation either as a means of computing the noise outright or as a model for unresolved noise sources, the selection of the best acoustic analogy comes down to the same two issues discussed by Doak (1972): accurate enough inversion of L and representation of S. Of these, the inversion of L can usually be better understood via the theory of linear equations. Convolution of S with a Green's function is viable when one is available for L. For more complex L, a numerical solution of the adjoint Green's function can be used to compute the far-field sound (Bodony & Lele 2003). This is efficient when the sound from many source points is needed at a limited number of points in the far field. If the sound is needed everywhere, then a direct solution is another viable means (e.g., Freund et al. 2005). A problem arises when solutions of $L\mathbf{q} = 0$ can grow large, as when L includes an inflectional free shear flow. Analytical treatments exist to suppress these homogeneous solutions, but they are challenging to implement (see discussion of Agarwal et al. 2004). In some cases, the phase velocity of the eigenmodes can be used to eliminate them if one has access to the wave number–frequency makeup of the source field (e.g., Colonius et al. 1997). Others have proposed suppressing them by removing particular terms in L that support instability modes but also appear to have only a weak effect on radiated sound (Bogey et al. 2002), or by imposing time periodicity (Agarwal et al. 2004). The adjoint Green's function methods are not free of such complications. If the flow is linearly receptive to disturbances propagated in the computation of the adjoint, then

adjoint instability modes will also be excited, which will potentially cause difficulties in predictions. When diffraction by a spreading base flow is included in L, the resulting homogeneous solutions are better behaved because instability modes are eventually damped downstream (Goldstein 2003). Recently, it was proposed that instead of being suppressed in the solutions, the instability solutions should be incorporated into a unified theoretical framework, which seems able to explain some key features of turbulent jet noise (Goldstein & Leib 2005).

Sensitivity to S, and in particular unavoidable errors in S due to numerical approximations or modeling assumptions, are less well understood. Because of the energy mismatch discussed in Section 2.2, it is possible that small errors in S can lead to disproportionately large or overwhelming errors in the far-field sound when $L\mathbf{q} = S(\mathbf{q})$ is solved. It can be speculated that the closer S is to a true noise source—that is, the less propagation physics lumped into it—the more likely relative errors in S will be reflected by similar relative errors in the far-field sound (Freund et al. 2005, Goldstein & Leib 2005). Preliminary empirical results suggest that this is the case for certain artificially introduced time-dependent errors (Freund et al. 2005), but more investigation is warranted for both this case and the case where the acoustic analogy is used with a statistical sound-source model.

3.2. Lighthill's Theory and Numerical Evaluation

Although it suffers from the source-propagation ambiguity discussed above, the Lighthill equation (Equation 1) remains the most widely used acoustic analogy. Its use is particularly justified at low Mach numbers where these ambiguities diminish and additional approximations can make it analytically more tractable. The last two terms in the Lighthill stress tensor T_{ij} are sometimes regrouped into an entropy-like term $(p - c_0^2\rho)\delta_{ij}$ and a viscous stress term. The viscous term is generally negligible because of its extremely inefficient octupole nature as a noise source (Crighton 1975) except when acted on a surface (see discussion in Section 3.3.2), and has been successfully neglected for even a $Re = 2000$ turbulent jet (Colonius & Freund 2000). The entropic term is also often thought to be small in absence of strong temperature inhomogeneities, but has also been found important for low-angle radiation from a nearly uniform temperature turbulent jet (Freund 2003). The remaining source term $T_{ij} \approx \rho u_i u_j$ can be computed based on compressible flow equations or, if the flow Mach number is small, their incompressible approximation. In the limit of low Mach number and a compact vorticity region, the validity of Lighthill's analogy has been shown using matched asymptotic expansions (Crow 1970). In general engineering flows with expansive regions of unsteadiness, however, the Lighthill theory or any other acoustic analogy should be viewed in the modeling framework and applied with caution. Although its derivation is exact, approximations and assumptions are invariably built into the solution process, which, if used improperly, can lead to erroneous results.

For an unsteady flow in an unbounded domain, a closed form "solution" to the Lighthill equation can be written as

$$\rho(\mathbf{x},t) = \frac{1}{4\pi c_0^2}\int_V \frac{1}{r}\left[\frac{\partial^2}{\partial y_i \partial y_j}T_{ij}(\mathbf{y},\tau)\right]_{\tau=t-r/c_0} \mathrm{d}^3\mathbf{y}$$
$$\approx \frac{1}{4\pi c_0^4}\int_V \frac{r_i r_j}{r^3}\frac{\partial^2}{\partial t^2}T_{ij}\left(\mathbf{y}, t-\frac{r}{c_0}\right)\mathrm{d}^3\mathbf{y}, \quad (2)$$

where $r = |\mathbf{x}-\mathbf{y}|$ is the distance between an observation point $\mathbf{x}$ and a source position $\mathbf{y}$, and $r_i = x_i - y_i$. The second expression in Equation 2 is obtained from the first one by applying the chain rule and the divergence theorem, coupled with the acoustic far-field approximation $r \gg \lambda$. If, in addition, $r \gg L_s$ (the characteristic size of the source region), r and r_i in the prefactor of Equation 2 can be approximated by $|\mathbf{x}|$ and x_i, respectively, and moved outside of the volume integral. The second expression is advantageous for numerical evaluation because the quadrupole nature of the source terms is explicit. By contrast, the first expression represents the source terms as monopoles, and thus requires the numerical procedure to provide the intricate cancellation of various source elements that is necessary for the quadrupole character to emerge. Crighton (1988, 1993) provides an illuminating discussion of how such a misrepresentation coupled with a lack of numerical accuracy can lead to gross overestimation of sound. This problem is particularly acute at low Mach numbers, because the numerical errors in the monopole formulation are amplified by the monopole scaling $\sim M^2$ relative to quadrupole scaling $\sim M^4$. At high subsonic or supersonic Mach numbers, the source representation becomes less critical due to the vanishing scale separation and larger acoustic amplitudes. A numerical comparison of the two formulations in Equation 2 was performed by Bastin et al. (1997) for the noise of a planar jet. At $M = 0.5$, the monopole formulation overpredicts the far-field sound pressure level (SPL) by up to 30 dB. The discrepancy is much reduced for a $M = 1.33$ jet, but remains significant at low frequencies and certain radiation angles.

It is tempting to solve the Lighthill equation directly on a mesh when dealing with complex geometries. However, this is equivalent to the monopole integral formulation and is therefore inadvisable for low-Mach-number flows, unless particular care is taken. Oberai et al. (2000, 2002) developed a variational formulation of the Lighthill equation in which the equivalence of the two integrals in Equation 2 is exactly preserved by their particular discretization. The far-field pressure agreed with that obtained using Curle's (1955) dipole solution in the low-frequency (compact airfoil) limit and exhibited the correct edge-scattering characteristics in the high-frequency (long chord length) regime.

A matter of practical concern in computation is where the formally infinite volume integral in Equation 2 can be truncated. In theory, it covers the entire unsteady region, including contributions from both hydrodynamic and acoustic perturbations. If the source terms do not decay sufficiently rapidly toward the computational boundaries, then special treatment is required to ensure convergence of the integral. The approximate Lighthill stress must be quadratic in fluctuating velocities at the boundary. If there is a uniform mean velocity (free-stream velocity) U_0 at the boundaries, linear "source" terms can be removed by using a reference frame that moves with the flow, leading to a convected wave equation and source terms defined in terms of the excess velocity $u - U_0$, as in the studies of Wang et al. (1996a) and Oberai et al. (2000).

However, in many flows of practical interest, such as jets and wakes, the unsteady flow region is extensive although the physical source of sound is of limited extent. Simple truncation of the source terms at the integration boundary creates spurious sound, which can contaminate the acoustic prediction (Crighton 1993). This issue is related to, yet different from, the spurious reflection of sound in direct computations (see Section 4.1), where nonreflective boundary conditions are required. Ad hoc techniques are available to remove the artificial boundary noise. These typically involve a modification of the source terms, such as using a ramp function to slowly damp out the source terms toward the boundary (Oberai et al. 2000). Wang et al. (1996a) demonstrate that, in the context of Lighthill's equation, the spurious boundary noise is due to the time variation of Lighthill stress fluxes across the boundary. They derived a correction based on a frozen eddy assumption (Taylor's hypothesis), which successfully removed the spurious noise arising from truncations of a wake vortex street (Wang et al. 1996a) and the wavy disturbances surrounding a transitional wave packet in a boundary layer (Wang et al. 1996b). Extension to other acoustic analogies can be easily made (Avital et al. 1999).

3.3. Effect of Solid Boundaries

When rigid and stationary surfaces are present in the flow, the solution to the Lighthill equation can be written as (Goldstein 1976),

$$\rho(\mathbf{x},t) = \frac{1}{c_0^2}\int\int_V T_{ij}\frac{\partial^2 G}{\partial y_i \partial y_j}\,\mathrm{d}^3\mathbf{y}\,\mathrm{d}\tau - \frac{1}{c_0^2}\int\int_S n_j\,p_{ij}\frac{\partial G}{\partial y_i}\,\mathrm{d}^2\mathbf{y}\,\mathrm{d}\tau, \tag{3}$$

where $G = G(\mathbf{x}, t; \mathbf{y}, \tau)$ is Green's function, and n_j are components of the outward pointing (into the fluid) unit normal of the surface S. If the free-space Green's function is used, Equation 3 becomes Curle's (1955) solution to the Lighthill equation, which takes the following form in the acoustic far field:

$$\begin{aligned}\rho(\mathbf{x},t) \;\approx\; & \frac{1}{4\pi c_0^3}\int_S \frac{r_i}{r^2}\frac{\partial}{\partial t} n_j\,p_{ij}\left(\mathbf{y}, t-\frac{r}{c_0}\right)\mathrm{d}^2\mathbf{y} \\ & + \frac{1}{4\pi c_0^4}\int_V \frac{r_i r_j}{r^3}\frac{\partial^2}{\partial t^2} T_{ij}\left(\mathbf{y}, t-\frac{r}{c_0}\right)\mathrm{d}^3\mathbf{y}.\end{aligned} \tag{4}$$

3.3.1. Choice of Green's function. In numerical evaluations, the applicability of Curle's integral depends on the size of the solid object and whether the source field is from a compressible or incompressible calculation. If the solid body is small relative to the acoustic wavelength, the effect of the body on sound propagation is negligible, and Curle's surface integral predicts a compact dipole, which at low Mach numbers dominates the volume quadrupole radiation. In this case, p_{ij} from either compressible or incompressible flow calculations can be used on S because the contribution from compressibility effects is $O(M^2)$ relative to the hydrodynamic contribution.

If the solid object is not acoustically compact, its presence is felt by not only the hydrodynamic field but also the acoustic waves, resulting in a more complex scattering field without a multipole character. To account for the surface reflection

of acoustic waves, the correct hard-wall boundary condition must be satisfied by the acoustic components of the flow. This can be achieved in two ways. If the source field is obtained from a compressible flow calculation, it already satisfies the appropriate acoustic boundary conditions, and hence Curle's solution is valid even though it utilizes the free-space Green's function. If, on the other hand, the source field is from a less expensive incompressible flow calculation, the acoustic boundary condition needs to be imposed when solving for the sound, which necessitates the use of a Green's function tailored to the specific geometry in consideration.

Analytical Green's functions for hard-wall boundaries are unavailable except for the simplest geometries, such as an infinite plane and semi-infinite plane (Goldstein 1976). In complex geometries, computation of the complete Green's function is generally expensive because it is a function of both source (**y**) and field (**x**) coordinates as well as time (or frequency). However, for a fixed far-field observation point **x**, the evaluation can be simplified by invoking the reciprocal theorem (Crighton 1975), which recasts the problem into one of finding the wave field near the body induced by an incident plane wave propagating from the direction of **x**. For relatively simple geometries, various levels of approximations for Green's functions are possible. For example, the half-plane Green's function (Ffowcs Williams & Hall 1970) has often been used for computing trailing-edge noise (Manoha et al. 2000, Wang & Moin 2000) on the basis that the airfoil is long and thin relative to the acoustic wavelengths of interest. However, its deficiency is highlighted in the case of a rectangular strut because the far-field solution depends on the placement of the half-plane relative to the strut (Manoha et al. 2000). This is due to the fact that although the strut (airfoil) thickness is negligible relative to the acoustic wavelength, it is finite compared to the flow scales and hence needs to be accounted for, which can be done following the analysis of Howe (1999) by approximating the Green's function in the frequency domain with a separable form: $G(\mathbf{x}, \mathbf{y}, \omega) \approx G_x(\mathbf{x}, \omega)\Phi(\mathbf{y})$. The first part, G_x, provides the acoustic directivity and can be approximated based on the ratio of the acoustic wavelength to the object size. The second part $\Phi(\mathbf{y})$ depends on the source distribution relative to the object, and is a potential flow solution: $\nabla^2\Phi = 0$.

3.3.2. The roles of surface pressure and shear stress. An illustrative example of the ambiguity common in acoustic analogies, even for nearly incompressible flow, involves the roles played by the surface pressure and shear stress on sound generation by flow above a rigid, planar boundary. Although Curle's equation (Equation 4), which is formally exact except for the well understood far-field approximation, predicts apparent surface dipoles due to the fluctuating stresses, the surface integral is generally divergent and therefore unsuitable for numerical evaluation. Powell (1960) reformulated Curle's solution to the Lighthill equation using the rigid wall (zero normal-gradient) Green's function, and demonstrated that the normal stress (pressure) dipoles are in fact specular images of the Reynolds stress quadrupoles, which leaves only the viscous shear stress terms in the dipole expression. The validity of the viscous stress dipoles as an acoustic source remains controversial (Crighton et al. 1992, Morfey 2003) and important for applying Lighthill's theory. If the viscous stress is indeed a noise source, it can dominate the sound radiation in the low-Mach-number

limit (Haj-Hariri & Akylas 1985, Landahl 1975, Wang et al. 1996b). However, it is also possible to interpret these terms as propagation effects. Howe (1979, 1995) concluded that their role is to attenuate the reflected acoustic waves, although his analysis does not seem to include the hydrodynamic (nonacoustic) contribution.

A number of recent computational studies have shed some fresh light on this issue. Shariff & Wang (2005) considered a simple model problem in which a small region in an infinite plane executes a low-Mach-number sinusoidal tangential motion, which induces an acoustically compact velocity/vorticity field in an otherwise quiescent fluid. Thus, the only force exerted on the fluid by the moving wall is the viscous shear stress. The numerical solution of the compressible Navier-Stokes equations in this case shows a dipole acoustic field in excellent agreement with the prediction using Powell's equation. This numerical experiment establishes hydrodynamic shear stress as a legitimate sound source, but does not address its relative importance in a realistic turbulent boundary layer. The latter issue was examined by Hu et al. (2002, 2003) with direct numerical simulations of turbulent plane channel and Couette flows. Their computations, which are incompressible, show that the wave number–frequency spectra of the shear stresses have finite values in the limit of zero wave number. Explicit far-field predictions using the DNS source data and Lighthill's theory suggest that the low-frequency dipole radiation due to the wall shear stress can exceed the quadrupole radiation at Mach numbers of $M \lesssim 0.1$.

In light of the new numerical evidence, it appears reasonable to treat fluctuating wall shear stress as source terms in boundary-layer noise calculations. The ultimate proof of its importance may require a compressible-flow DNS at low Mach number with sufficient accuracy to capture the dipole sound and delineate it from the quadrupole sound, which is extremely difficult. The mechanism for the wall shear-stress sound generation is explained by Herbert et al. (1999), Hu et al. (2003), and Morfey (2003) in terms of viscous scattering, by which the no-slip condition converts incident vortical disturbances in the viscous sublayer into outgoing sound waves. A comprehensive discussion of the effect of viscosity in the sound-generation process can be found in Morfey (2003).

3.3.3. Moving boundaries—Ffowcs Williams-Hawkings equation. The most general form of Lighthill's analogy is the extension developed by Ffowcs Williams & Hawkings (1969), which incorporates the effect of surfaces in arbitrary motion. The integral form of the Ffowcs Williams-Hawkings (FW-H) equation includes surface and volume integrals representing the sound due to the displacement of fluid by the body (thickness noise), unsteady loading, and quadrupole sources. It is at the heart of today's prediction methods for noise from rotating machines, such as helicopter rotors, fans, and propellers. Brentner & Farassat (2003) give a comprehensive review of its mathematical foundations, various integral formulations for computational evaluations, and efficient numerical algorithms, with applications to helicopter noise.

The integral formulation of the FW-H equation is derived based on the free-space Green's function, and therefore requires source data from compressible flow calculations if the surface is acoustically noncompact. In applying the FW-H equation, the volume quadrupole noise is negligible at low Mach numbers but becomes important

at transonic and supersonic Mach numbers. Its explicit evaluation can nonetheless be avoided if the FW-H equation is applied on a fictitious, permeable surface instead of the physical surfaces. The contribution of volume sources within the surface to sound radiation is then included in the surface source terms. This approach, which essentially treats the FW-H method in the same way as the Kirchhoff method (Farassat & Myers 1988), has gained popularity in recent years because of computational efficiency (Brentner & Farassat 2003). Comparisons of the permeable surface FW-H method and Kirchhoff method have been conducted in a number of configurations. Gloerfelt et al. (2003) show correct acoustic predictions from both methods compared with DNS data in the case of a two-dimensional subsonic cavity flow, even when the fictitious surfaces are close to the cavity surface (not entirely in the linear region). Brentner & Farassat (1998) and Singer et al. (2000), on the other hand, observe from calculations involving a hovering rotor and flow over a circular cylinder, respectively, that the permeable surface FW-H method is more robust. It can tolerate certain levels of flow nonlinearity on the surface, whereas the Kirchhoff surface needs to be placed in the linear wave regime to obtain accurate results.

4. COMPUTATIONAL METHODS AND APPLICATIONS

4.1. Basic Numerical Considerations for Direct Sound Computation

Special features of flow-sound problems have demanded special numerical considerations, most of which stem from the very low energy content of the radiated noise relative to the unsteady flow. Because of this energy mismatch, small errors in the unsteady flow, which would otherwise be benign, have the potential to ruin predictions of the radiated sound. The result is that the computational aeroacoustics community, more than most disciplines, has been acutely aware of two issues in particular.

The first issue is the need for accurate boundary conditions. Most flows of interest have extensive unsteady hydrodynamics in at least one coordinate direction. Jets, for example, extend downstream of their origin well beyond what would be practical to include in a computation, so boundary conditions are needed that can absorb flow disturbances as they exit the computational domain without causing excessive acoustic reflections. Colonius (2004) provides a thorough review of these issues and available resolutions.

The second issue is the spatial resolution of numerical schemes, often quantified as the number of points per wavelength needed to represent advection or wave propagation to within some error threshold. With the exception of Fourier spectral methods, discretizations induce artificial dispersion and, in some cases, dissipation. In practice, this is primarily due to the spatial discretization, whether it is finite difference, volume, or element based. The need for special attention in this regard for flow-noise computations is often attributed to the necessity of propagating sound waves over large distances, but in most noisy flows of practical interest, the flow itself usually presents a greater resolution challenge. The efficient analytical and semianalytical techniques discussed in Section 3.3.3 can typically be applied within an acoustic wavelength or

two of the flow and used to calculate the far-field noise, which removes the need for long-range propagation of acoustic waves on a mesh. In DNS, the viscous length scale is usually much smaller than any sound wavelengths and is therefore commonly more demanding in terms of mesh points. Care must be taken to ensure resolution of all the relevant scales. Using more and more points is the brute force way to ensure this, but high-order finite difference methods typically have better resolution properties than low-order methods for the same computational expense, and for the same formal-order compact schemes generally have better resolution than explicit finite differences (Lele 1992). For most methods with high formal order, well resolved flow features are more accurately represented than necessary, which has motivated several efforts to sacrifice this formal order in favor of an expanded range of wavelengths that are represented to within some error threshold (Lele 1992, Tam & Webb 1993). Colonius & Lele (2004) provide a chart for selecting a finite-difference method from some available schemes to minimize computational expense given an accuracy target. Time discretization has, in general, not been afforded as much attention as spatial discretization. Fourth-order Runge-Kutta schemes have been particularly popular in application, but resolution-optimized schemes have also been developed (Hu et al. 1996). Implicit schemes are sometimes used for flow over solid objects due to the small mesh spacing required to resolve the viscous boundary layers.

4.2. Direct Numerical Simulation of Flow Noise

For scientific investigation of flow noise, DNS is usually used to avoid modeling approximations. The compressible flow equations are discretized and solved on a mesh with methods that have well understood numerical errors so their effect can be reduced to an acceptable level. The resulting simulations provide a detailed (all space-time information is available) description of flow and, with sufficient accuracy, the concomitant sound. Therefore, DNS provides a remarkably "clean" means of studying aerodynamic sound phenomena. The disadvantage of this approach is its well-known Reynolds number limitation.

The first DNS of flow-generated sound was a study of the noise generated by a pair of two-dimensional co-rotating voriticies (Mitchell et al. 1992, 1995), which generate sound at primarily twice the rotation frequency of the system. The simulation database, which extended into the acoustic far field, permitted the first direct application of several acoustic analogies, showing that despite certain concerns voiced about aspects of their formal derivation (Crow 1970, Doak 1972), their evaluation (by convolution integral in this study) gave the correct noise. It also showed that accuracy concerns voiced early in efforts to compute flow-generated sound (Crighton 1988) were not insurmountable. More recent investigations of noise from compact regions of vorticity have included colliding axisymmetric vortex rings (Inoue et al. 2000) and more. Ran & Colonius (2004) studied sound generation by transition and turbulent decay of an initially laminar vortex ring. By tracking the temporal evolution of the far-field sound signature and the corresponding vortex-ring structure (**Figure 2**), the radiation characteristics of various linear and nonlinear instability modes, vortex breakdown, and turbulent decay were identified. Furthermore, they

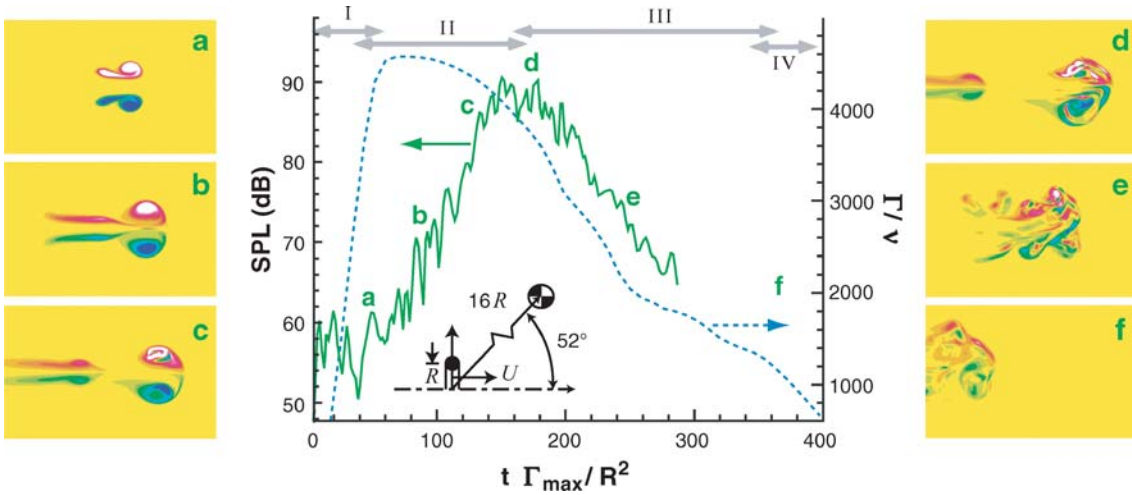

Figure 2

Sound generated by a turbulent vortex ring computed using DNS (Ran & Colonius 2004). Plotted in the middle is the temporal evolution of ensemble ($N = 15$) averaged far-field SPL (*solid line*) and total circulation (*dashed line*). SPL is measured at the point indicated on the diagram and the curve is shifted in time by the expected retarded time factor. In frames (*a*) to (*f*), iso-contours of vorticity (normal to plane) in a slice through the ring depict snapshots of one realization. The marked stages of evolution correspond to (I) vortex ring formation, (II) instability and early transition, (III) late transition and self-similar decay, and (IV) (nonphysical) exit from computational domain.

found a remarkable similarity between the high-frequency sound spectrum and that of a correspondingly low-Reynolds-number turbulent jet, which suggests a potentially universal character to the mechanisms.

The first investigation of the noise from an extensive region of unsteady hydrodynamics was reported by Colonius et al. (1997), who considered the noise generated by regular unsteady rollups and pairings in a two-dimensional mixing layer. The regular (nearly perfectly periodic) character of this flow facilitated detailed analysis of noise sources as defined by the Lilley equation (Goldstein 1976, Lilley 1974), but also made the flow acoustically inefficient (Wei & Freund 2005), which should be considered in interpreting the results. Although the feasibility of using this acoustic analogy was demonstrated, success depended on subtle features of the noise-source formulation. Common simplifications caused erroneous predictions, whereas the quadrupole source form of Goldstein (1984) showed excellent results. Somewhat surprisingly, given the nominally low Mach number of the flow ($M_1 = 0.5$ and $M_2 = 0.25$), a compact source approximation could not be made, which indicated that although acoustic analogy is a viable means of predicting noise, modeling their sources as quadrupoles must be done with caution.

The first DNS of a turbulent jet was reported by Freund et al. (2000). The Mach number was 1.92 and the flow was nearly isothermal, so the principal noise radiation was by Mach waves generated by supersonically advecting flow structures.

A special inflow boundary condition (Freund 1997) was used to "feed" turbulence from a streamwise periodic auxiliary simulation into the domain. Although the numerical solution was verified to accurately solve the compressible flow equations, the flow parameters were unfortunately not selected to match any particular experiment. Nevertheless, the database was used to investigate nonlinearity in the near acoustic field (Freund et al. 2000) and nonlinear mechanisms in the generation of Mach wave radiation from supersonic jets (Mohseni et al. 2002), and it was used in the first direct application of an acoustic analogy (Lighthill's) to a turbulent jet (Colonius & Freund 2000). Freund (2001) reported the first DNS of a subsonic ($M = 0.9$) turbulent jet, which matched the experimental conditions of Stromberg et al. (1980) and showed agreement with experiment for mean-flow development, noise directivity, and noise spectra. This database has been used to compute noise-source turbulence statistics, which were previously unavailable (Freund 2003), to investigate aspects of high-frequency noise interactions with jet turbulence (Freund & Fleischman 2002), and to examine the three-dimensional empirical eigenfunction of a turbulent jet as defined by various energy norms (Freund & Colonius 2002).

Manning & Lele (2000) and Suzuki & Lele (2003) employed DNS to study the physical processes responsible for generating screech noise using a model problem in which nonlinear shear-layer instability wave disturbances interact with an imposed, stationary, compression wave and its reflection (Mach wave system) in the supersonic part of the flow. The self-excitation of the shear layer is suppressed with an "absorbing" boundary-zone treatment. As large-scale shear-layer vortices convect past the interaction region, the tip of the compression wave oscillates significantly. When the so-called braid region passes over the compression wave tip, a part of this wave leaks across the shear layer toward the ambient region, initiating a sharp cylindrical compression wave. Refraction of this wave back into the supersonic flow can also be observed as an upstream traveling Mach wave within the supersonic flow. Suzuki & Lele (2003) showed that many features of the DNS can be reproduced using geometrical acoustics.

4.3. Large-Eddy Simulation

4.3.1. Methodology and applications. Barring any dramatic improvements in RANS-based noise models, LES offers the best promise in the foreseeable future for noise prediction at Reynolds numbers of practical interest. It copes with the well-known Reynolds number limitation of DNS by only explicitly representing the large turbulence scales in the flow, and models the effect of the smaller scales. The mathematical formalism for LES is established through a spatial filtering operation applied to the Navier-Stokes equations, which results in unclosed subgrid-scale (SGS) stress terms. Because the small-scale motions are more universal than the large-scale motions, SGS modeling is expected to be more robust than turbulence modeling in the RANS context. The prevailing closure strategy is based on the Smagorinsky (1963) eddy viscosity model. In the early 1990s, a dynamic procedure for computing the model coefficient from the resolved velocity field was developed, which requires no adjustable constant and near-wall damping function (Germano et al. 1991, Lilly

1992), and thus marks a major improvement in the robustness and accuracy of LES. In compressible flows, SGS flux terms are also present in the continuity and energy equations, which can be modeled in an analogous way (Moin et al. 1991). Other popular SGS models include the scale similarity model (Bardina et al. 1983) and mixed models, approximate deconvolution model (Stolz & Adams 1999), and multiscale LES (Hughes et al. 2001), to name a few.

The accuracy of LES depends strongly on the underlying numerical algorithms. Numerical dissipation, which is prevalent in RANS applications, can artificially damp turbulent eddies and their associated sound spectra, particularly in the high- and intermediate-frequency ranges. Hence, the development of nondissipative or low-dissipative numerical algorithms has been a major component of LES research (Moin 2002).

The maturation of LES techniques and increasing computational power have enabled the computation of flow-generated sound under realistic experimental flow conditions. Wang & Moin (2000) applied incompressible LES in conjunction with Lighthill's theory to simulate the trailing-edge aeroacoustic experiment of Blake (1975), which involves flow over a flat strut with an asymmetric trailing edge at chord Reynolds number of 2.1×10^6. To reduce computational expense, only the aft section of the strut was included in the simulation domain, and realistic turbulent boundary-layer inflow data were provided by separate simulations. The acoustic Green's function was approximated by that for a thin half-plane. Reasonable agreement with experimental data (Blake 1975, Blake & Gershfeld 1988) was obtained for velocity statistics, frequency spectra of surface pressure fluctuations, and the far-field sound spectra. More recently, Wang et al. (2004) further validated the LES approach for computing the spatio-temporal characteristics of unsteady pressure on a model fan blade at Reynolds number of 1.5×10^5. Other LES predictions of trailing-edge noise have been performed by Manoha et al. (2000) for a flat strut with a blunt trailing edge and by Oberai et al. (2002) for an Eppler 387 airfoil. All the above flows are at a low Mach number, and the incompressible Navier-Stokes equations were used for the source-flow simulations.

LES predictions of jet noise were recently attempted based on the compressible Navier-Stokes equations. For instance, Bogey et al. (2003) computed the sound field of a Mach 0.9 jet at a Reynolds number of 6.5×10^4 obtained directly from LES and validated their flow and sound statistics with experimental data. In recent work, Bodony & Lele (2005) conducted a systematic investigation of LES's predictive capability for jet noise. A series of jet simulations were carried out at three different Mach numbers ($M_j = 0.5, 0.9$, and 1.5) for the cold and hot jets studied experimentally by Tanna (1977). The Reynolds numbers considered range from 1.3×10^4 to 3.36×10^5. The predictions are generally in agreement with experimental data, although some discrepancies are observed depending on the jet operating conditions and are attributed to resolution limitations, which prevent the inclusion of the realistic turbulent near-nozzle shear layers found in laboratory jets. As shown recently by Bogey & Bailly (2005a), inflow conditions, particularly the spatial structure of inflow disturbances, can significantly impact the development of the jet flow and the emitted sound predicted by LES. The specification of turbulent inflow forcing with

realistic broadband excitation, but without spurious noise, remains an important issue requiring further work.

4.3.2. Effect of subgrid-scale modeling on sound prediction. Using the Lighthill framework for discussion, the effect of SGS modeling can be illuminated by the following decomposition of the Lighthill stress tensor:

$$T_{ij} \approx \rho_0 u_i u_j = \underbrace{\rho_0 \overline{u}_i \overline{u}_j}_{T_{ij}^{LES}} + \underbrace{\rho_0 (\overline{u_i u_j} - \overline{u}_i \overline{u}_j)}_{T_{ij}^{SGS}} + \underbrace{\rho_0 (u_i u_j - \overline{u_i u_j})}_{T_{ij}^{MSG}}, \quad (5)$$

where the overbar denotes spatial filtering and a constant density is assumed. For higher-Mach-number flows, the spatial filtering can be density weighted in the sense of Favre filtering (Moin et al. 1991) or, alternatively, applied to density as well (Bodony & Lele 2005). The first term, T_{ij}^{LES}, represents the Lighthill stress evaluated from the resolved velocity field, and the second term, T_{ij}^{SGS}, is the subgrid-scale contribution to the Lighthill stress at resolved scales. The combination of these two terms, $\overline{T}_{ij} = T_{ij}^{LES} + T_{ij}^{SGS}$, represents all the information that can be extracted from an LES source field. The subgrid-scale term is, however, generally inaccurate and not fully available from many popular SGS models such as the Smagorinsky-type model, in which the trace of the SGS stress tensor is absorbed into pressure. The last term in Equation 5, T_{ij}^{MSG}, represents the unresolved "missing" part of the Lighthill stress, which can only be modeled. A common practice in today's Lighthill-based calculations is to use only the first term in Equation 5 to represent the sound source.

Despite the growing interest in LES for sound prediction, not enough attention has been paid to the accuracy of the method and, in particular, the effect of SGS models. Piomelli et al. (1997) investigated the effect of small scales on the Lighthill stress and its second time derivative by an a priori analysis of a channel flow DNS database. However, it is difficult to draw conclusions about the sound field without actually computing it, because the Lighthill stress or its Eulerian time derivatives are not directly correlated with sound generation (passive convection of eddies in a uniform flow generates no sound but significant T_{ij} and $\partial^2 T_{ij}/\partial t^2$). Seror et al. (2000, 2001) performed a priori and a posteriori tests of the contributions of the three terms in the Lighthill stress decomposition (Equation 5) to sound production for decaying and forced isotropic turbulence. The missing-scale contribution was found to be negligible with typical cut-off wave numbers used in LES, whereas the SGS contribution was quite sizable. The latter was largely recovered by using the scale-similarity SGS model (Bardina et al. 1983) to compute T_{ij}^{SGS}. He et al. (2002, 2004) examined the SGS modeling effect on the velocity space-time correlations, which are related to the radiated sound intensity by a statistical formulation of Lighthill's theory. For decaying isotropic turbulence, their analysis indicates that the accuracy of space-time correlations is determined by that of the instantaneous energy spectra. The performance of several SGS models was evaluated in terms of space-time correlations, and the dynamic model in conjunction with the multiscale LES procedure was the most accurate. Note that the above analyses are all for homogeneous and isotropic turbulence, which is very different from realistic noisy flows with shear and other

complex effects. In the case of jet noise, Bogey & Bailly (2005b) noted that the LES solutions obtained using the dynamic SGS model were quantitatively similar to those obtained at lower Reynolds numbers without explicit SGS modeling but with "selective filtering" to remove small scales near the grid cut-off wave number. They therefore concluded that the effective Reynolds number of the jet was lowered by the eddy viscosity model, and opted for high wave number filtering alone in their jet LES (Bogey & Bailly 2005a,b). A similar approach was adopted by Shur et al. (2005a,b), whose simulations included a variety of physical effects important to aircraft jet engines. However, this approach to SGS modeling is not based on the physics of small-scale turbulence and its robustness, say in wall-bounded flows, is not known. More research is needed to understand and quantify the errors introduced by SGS modeling as well as numerical errors in practical aeroacoustic and hydroacoustic predictions.

Depending on the flow and mesh resolution, the sound of missing scales can be important and hence needs to be modeled. This is particularly the case in LES of jet noise, where the high-frequency spectral components not captured by current LES grids (Bodony & Lele 2005) are highly annoying to the ear and heavily weighted in noise regulations. In many situations, such as in the noise radiation from dual-stream jet of a turbo-fan engine, the noise generated by the missing scales is expected to propagate through significant regions of nonuniform flow, which may be best captured with explicit refraction effects included in the model. Goldstein's generalized acoustic analogy is the basis of the SGS noise modeling approach developed by Bodony & Lele (2003) and applied in their a posteriori LES study of the noise from a turbulent mixing layer (Bodony 2004). They used the DNS data of the same flow to validate the results. Numerically computed adjoint solutions were used to relate the source-term statistics to the far-field sound spectral levels. The source-term statistics were estimated by applying the approximate deconvolution method (ADM) of Stolz & Adams (1999) to the LES data as a post-processing step. Even though good agreement with the DNS data was obtained, the study showed two limitations of this procedure. Reconstruction of source-term statistics using ADM is computationally expensive (because data processing in space-time is required), and ADM extrapolation is significantly band-limited. Use of adjoint solutions (Bodony & Lele 2003) for SGS noise modeling becomes attractive if statistical models of the missing-scale source terms are developed and used. SGS noise modeling remains an area of new research.

4.4. RANS and LES/RANS Hybrid Methods

In practical aeroacoustic applications, particularly those with solid boundaries, even LES is often not feasible. A major obstacle to LES of high-Reynolds-number flows is the stringent near-wall grid resolution requirement, which is nearly comparable to DNS (Piomelli & Balaras 2002). Small but dynamically important eddies near the wall cannot be modeled adequately on a coarse grid by current SGS models. Furthermore, in many external flows with extensive thin boundary layers, it is not even feasible for LES to resolve the turbulent eddies based on the outer scales (Spalart et al. 1997).

To overcome these difficulties, two related approaches, which incorporate RANS modeling elements into LES at different levels, have recently been actively pursued.

The first approach, pioneered by Deardorff (1970), involves a combination of LES with a wall-layer model. The dynamics of the near-wall structures, typically in the viscous sublayer, buffer layer, and a lower portion of the log layer, is modeled using a RANS-type model, and its effect on the outer flow is provided to the LES as a set of approximate boundary conditions, often in the form of a shear stress. The complexity of the RANS model can vary from a simple algebraic relation (instantaneous log law) to turbulent boundary-layer equations, as discussed in detail in the review articles of Cabot & Moin (2000) and Piomelli & Balaras (2002). If part of the Reynolds stress is represented in the wall model equations, the RANS eddy viscosity needs to be reduced to match the total stress at the RANS/LES interface (Cabot & Moin 2000, Wang & Moin 2002). Wang & Moin (2002) applied this method to the trailing-edge flow studied previously using full LES and obtained comparable low-order velocity statistics at a small fraction of the original computational cost. The frequency spectra of surface-pressure fluctuations were also well predicted.

The second approach, proposed by Spalart et al. (1997, also see Travin et al. 2000), is essentially an extension of the LES wall modeling concept. Instead of using RANS for the near-wall layer, however, the RANS region is extended to the entire attached boundary layer, and LES is used to treat the separated region of the flow field (hence the name detached-eddy simulation, or DES). The switch from RANS to LES is controlled by the local grid spacing relative to distance to the wall, and therefore grid design is crucial to the solution quality. DES can be easily implemented in an existing RANS code with a small modification of the turbulence model; however, the strong numerical dissipation inherent in typical RANS algorithms is detrimental to the LES region, and the artificial transition from RANS to LES requires special attention. The DES technique is designed for massively separated flows and has been employed to predict the noise from such flows. Hedges et al. (2002) computed the noise radiated from an aircraft landing gear model using DES and the FW-H equation and compared results with those from unsteady RANS calculations. DES captured more details of the wake flow and a noise spectrum with a broader peak and higher-frequency contents. However, there were no experimental data available for a quantitative assessment of the DES results.

In the hierarchy of time-accurate simulation methods, the unsteady RANS (URANS) approach provides the lowest level of flow detail and accuracy. It can be effective in capturing large-scale fluid motions and the associated sound, but cannot provide broadband source information. There are some modeling ambiguities because turbulence models, mostly based on the concept of eddy viscosity, are developed for steady RANS calculations in which all the Reynolds stresses are modeled. The calculation of the plane-jet mixing noise by Bastin et al. (1997) was essentially based on URANS, which they called "semi-deterministic modeling." In the k-ε model employed, the turbulent viscosity constant was reduced to obtain the best time-periodic coherent structures in the jet. Shen & Tam (2000, 2002) combined a URANS approach with Euler equations to study jet screech. The URANS equations were solved with the k-ε model in the turbulent flow region and the Euler

equations were solved in the exterior region. This method reproduced the mode switching observed experimentally. Some recent URANS applications for airframe (slat, landing gear, wheel well cavity) noise predictions have been discussed by Singer & Guo (2004). Finally, steady RANS calculations are insufficient by themselves for sound predictions because of a lack of temporal information. Nonetheless, they have been combined with statistical models to provide statistical descriptions of acoustic source terms (Bailly et al. 1997, Khavaran & Bridges 2005, Tam & Auriault 1999).

5. FLOW-NOISE CONTROL

Computational techniques are becoming a viable tool for exploring noise-control concepts and strategies. Applications in this area recently began and will undoubtedly grow. Some very recent efforts in active and passive noise control are reviewed here briefly. The focus is on directly modifying the flow-noise sources, rather than introducing secondary sources (anti-sound), to achieve quieter flows. The latter approach was dealt with extensively in a recent review article (Peake & Crighton 2000).

Wei & Freund (2005) employed DNS and an adjoint method to explore means of noise control in a free shear flow and study the underlying physical mechanisms for the noise reduction. Using a two-dimensional randomly excited mixing-layer model for the near-nozzle region of a turbulent jet, the adjoint of the linearized compressible flow equations was forced by a measure of the radiated noise and solved backward in time to obtain the sensitivity of that noise to changes in control at the "splitter plate." Significant suppression of acoustic radiation in all directions and by up to 10 dB in the specific region targeted by the noise metric was found. Remarkably, the changes to the randomly excited mixing layer were nearly imperceptible: mean flow spreading, the kinetic energy, vortex pairings and so on were superficially unchanged (see **Figure 3**). Empirical eigenfunction analysis of the flow, however, showed that its energy is arranged into a more regular underlying wave-packet structure by the control, which would be acoustically less efficient. This view is confirmed by comparing to a harmonically (as opposed to randomly) excited mixing layer. The harmonically excited case, which was, of course, highly ordered from the start, matched the ordered character of the controlled randomly excited cases. It also could not be further quieted by the controller. Although successful in this two-dimensional flow, it remains unclear how effective such a mechanism might be in turbulent flows. Collis et al. (2002) used similar optimal control techniques to control the noise from a model blade-vortex interaction.

Compared with active flow control for noise reduction, an easier-to-implement approach is passive control by modifying the shapes of solid boundaries in the flow. This technique has been employed in many practical applications; for example, the use of serrated nozzles is effective in reducing jet noise (Bridges & Wernet 2002), but is currently developed for the most part based on trial-and-error iterations. The choice of shape parameters can be made systematic and efficient within an optimization framework in conjunction with reliable computational simulations of the source field. This approach was recently pursued by Marsden et al. (2004a,b; 2005) in the context of trailing-edge noise reduction.

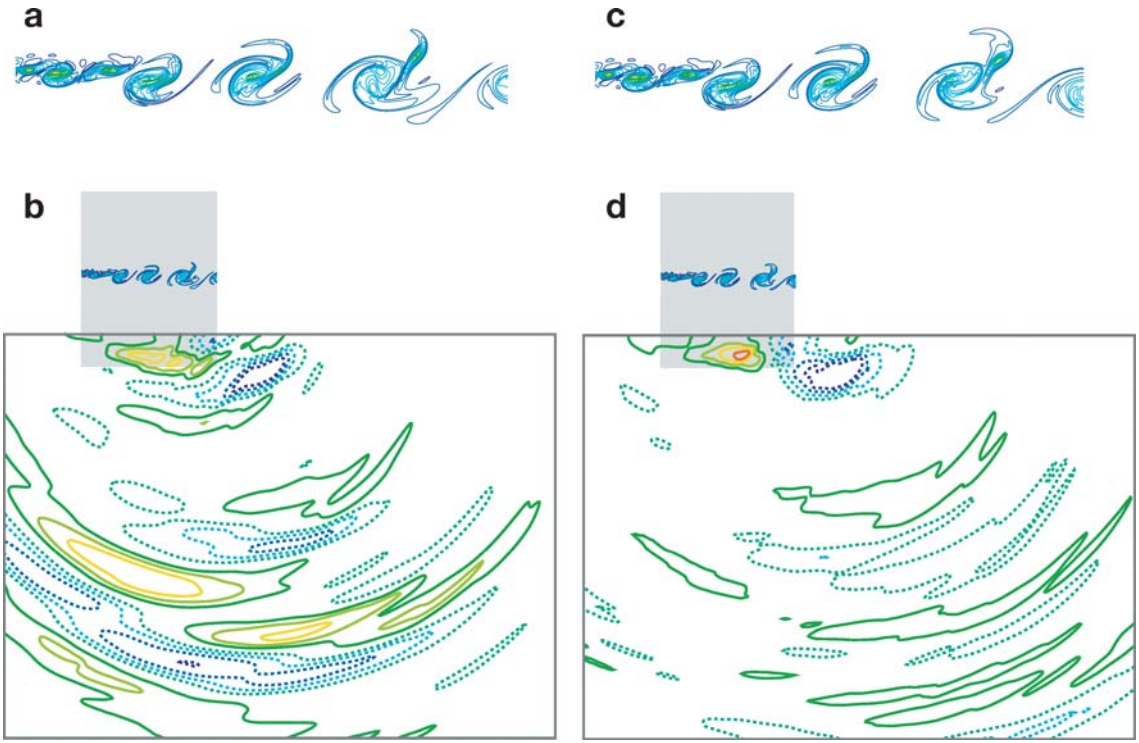

Figure 3

Optimal control of two-dimensional mixing layer noise. (*a*) visualizes the vorticity at a particular time before control with sound-field pressure contours shown in (*b*), and (*c*) visualizes the vorticity field at the same time after control with sound shown in (*d*). The pressure-contour spacing is $\Delta p = 0.001 p_\infty$ with the $p = 0$ contour omitted for clarity. Negative-valued contours are dashed.

The popular adjoint-based techniques for the full Navier-Stokes equations are difficult to use in unsteady flow problems on a large grid because of data storage and implementation issues. As a more general alternative, Marsden et al. (2004a,b) adapted an efficient derivative-free technique known as the surrogate management framework (Booker et al. 1999) to optimize the shape of an airfoil's trailing edge. The cost functions, targeted for reduction by the control, represented the radiated acoustic power based on Lighthill's theory and were evaluated from time-dependent Navier-Stokes simulations. The methodology was first successfully applied to suppress the noise of laminar vortex shedding from an acoustically compact airfoil with lift and drag constraints (Marsden et al. 2004b). The optimization resulted in significant reduction (as much as 70%) in acoustic power as well as novel airfoil shapes, with reasonable computational expense. To cope with the computational cost of extending to turbulent trailing-edge flow (Marsden et al. 2005), a method was developed that used RANS calculations for constraint evaluation and LES for cost function evaluation. The optimization was again successful: At a chord Reynolds number of

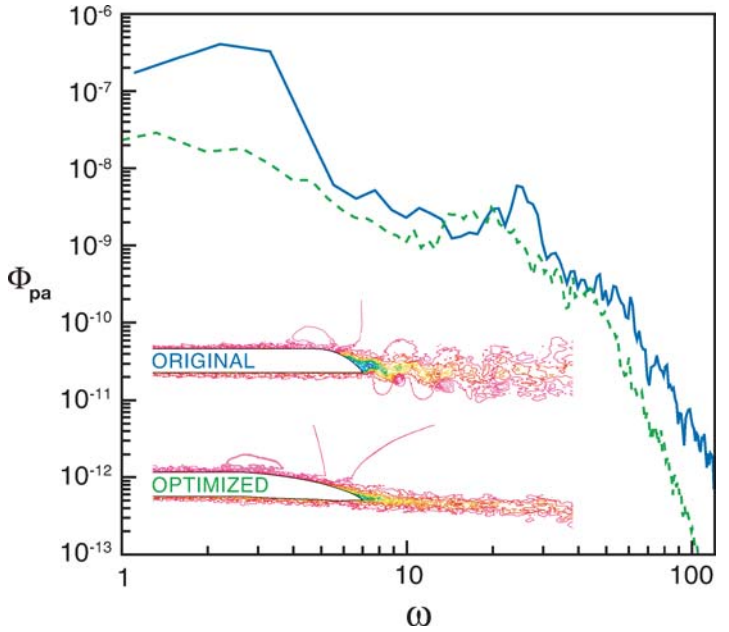

Figure 4

Dimensionless sound-pressure spectra as a function of frequency before (*solid line*) and after (*dashed line*) trailing-edge shape optimization. Dependence on observer location has been absorbed into the spectra based on the far-field directivity of a half-plane. Insert: Snapshots of streamwise velocity contours in a spanwise plane for the original and optimized trailing edges.

1.9×10^6, the trailing-edge noise power was reduced by 89%, which came about largely by suppressing vortex shedding at low frequencies in this turbulent flow, as shown in **Figure 4**. The higher-frequency noise was reduced as well, due to a subtle change of the lower-surface shape and its boundary layer near the trailing edge.

6. CLOSURE AND OUTLOOK

Flows encountered in engineering applications tend to be complex, often involving multiple physical and chemical processes such as transition to turbulence, boundary-layer separation, shock-wave/boundary-layer interaction, fluid-structure interaction, two-phase flows, chemical reactions, and so on. Additionally, the flows occur in close proximity of solid surfaces, which at times are geometrically complex.

Successful prediction of the flow-generated sound in such a context requires a good understanding of the unsteady processes in the flow system as a whole. It is generally not feasible to capture all of the dynamical processes at high fidelity. Some flow regions dominate the sound generation and others propagate and redistribute it. Accordingly, the fidelity at which the unsteady flow processes in various regions are to be computed needs to be selected. Computational tools that enable such hybrid simulations of complex flows are still in their infancy. Efforts at combining URANS and LES are actively being pursued, and so are the efforts to embed

locally refined grids for accurate flow- or geometric-feature capturing. Apart from the advances in numerical algorithms for flow simulations, the revolution in massively parallel computer hardware and parallel computing software is redefining the state of the art in computational sciences. Computer hardware with 100,000 processors to reach near-petaflop performance (1000 trillion floating-point operations per second), such as the Blue Gene/L at Lawrence Livermore National Laboratory, are being assembled. Although the capabilities available to a scientist or an engineer are more modest, dedicated teraflop performance is likely to be available with modest means. Simulation-based optimization and design become increasing realistic with the availability of such computer hardware.

It is tempting to target the development of computational methods toward the aeroacoustic prediction of real-life engineering systems and impact their design. But this does not exclusively require accurate noise predictions for the complete hardware. Effective solutions can often be found by decomposing the complex flow-sound system into simpler subelements. Fundamental studies of generic problems highlight the physics of sound generation and bring out technical issues that must be satisfactorily addressed for a proper modeling and scaling of the output sound power, its directivity, and its spectral makeup. Computations also provide an ability to simulate physical phenomena in ways that cannot be reproduced in the lab. It is possible to consider both physical and unphysical changes in the mathematical model being solved, and to formulate and solve inverse problems to obtain sensitivities of the radiated sound to flow parameters, flow features, boundary conditions, and geometric parameters. It is likely that new intrinsically quiet configurations will be discovered in this way.

Unsteady flow processes are at the core of predicting flow-generated sound. To the extent empirical models are used to predict the flow, including turbulence phenomena, the prediction of the radiated sound would remain empirical. There are good reasons to expect that properly validated hybrid simulation methods will remove much of this empiricism. These developments require careful verification that numerical errors are small and validation that the solution is in good agreement with laboratory or full-scale data. The latter requires high-quality data on the unsteady flow and the sound. There is surprisingly little data of this kind, but the computer hardware revolution is also enabling new diagnostics for flow and sound measurements. Integrated use of computational and experimental tools will be necessary to explore new designs, which must not only meet ever more stringent community noise regulations, but also be environmentally friendly and economically viable.

ACKNOWLEDGMENTS

MW acknowledges sustained support from ONR, JBF from AFOSR and NASA, and SKL from Aeroacoustics Research Consortium and Boeing, for research in this area.

LITERATURE CITED

Agarwal A, Morris PJ, Mani R. 2004. Calculation of sound propagating in nonuniform flows: suppression of instability waves. *AIAA J.* 42(1):80–88

Avital EJ, Sandham ND, Luo KH. 1999. Calculation of basic sound radiation of axisymmetric jets by direct numerical simulations. *AIAA J.* 37(2):161–68
Bailly C, Lafon P, Candel S. 1997. Subsonic and supersonic jet noise predictions from statistical source models. *AIAA J.* 35(11):1688–96
Bardina J, Ferziger J, Reynolds WC. 1983. Improved turbulence models based on large-eddy simulation of homogeneous, incompressible, turbulent flows. *Tech. Rep. TF-19*, Dep. Mech. Eng., Stanford Univ., Stanford, CA
Bastin F, Lafon P, Candel S. 1997. Computation of jet mixing noise due to coherent structures: the plan jet case. *J. Fluid Mech.* 335:261–304
Blake WK. 1975. A statistical description of pressure and velocity fields at the trailing edge of a flat strut. *Tech. Rep. No. 4241*, David Taylor Naval Ship Res. Dev. Cent., Bethesda, MD
Blake WK. 1986. *Mechanics of Flow-Induced Sound and Vibration*, Vols. I, II. London: Academic. 974 pp.
Blake WK, Gershfeld JL. 1988. The aeroacoustics of trailing edges. In *Frontiers in Experimental Fluid Mechanics*, ed. M Gad-el-Hak, pp. 457–532. New York: Springer-Verlag. 532 pp.
Bodony DJ. 2004. *Aeroacoustic prediction of turbulent free shear flows.* PhD thesis. Dep. Aeronaut. Astronaut., Stanford Univ., Stanford, CA
Bodony DJ, Lele SK. 2003. A statistical subgrid scale noise model: formulation. *AIAA/CEAS Pap. 2003-3252*
Bodony DJ, Lele SK. 2005. On using large-eddy simulation for the prediction of noise from cold and heated turbulent jets. *Phys. Fluids.* 17(8):085103
Bogey C, Bailly C. 2005a. Effects of inflow conditions and forcing on subsonic jet flows and noise. *AIAA J.* 43:1000-7
Bogey C, Bailly C. 2005b. Decrease of the effective Reynolds number with eddy-viscosity subgrid-scale modeling. *AIAA J.* 43:437–39
Bogey C, Bailly C, Juvé D. 2002. Computation of flow noise using source terms in linearized Euler's equations. *AIAA J.* 40(2):235–43
Bogey C, Bailly C, Juvé D. 2003. Noise investigation of a high subsonic, moderate Reynolds number jet using a compressible large eddy simulation. *Theor. Comput. Fluid Dyn.* 16(4):273–97
Booker AJ, Dennis JE, Frank PD, Serafini DB, Torczon V, Trosset MW. 1999. A rigorous framework for optimization of expensive functions by surrogates. *Struct. Optim.* 17(1):1–13
Brentner KS, Farassat F. 1998. An analytical comparison of the acoustic analogy and Kirchhoff formulation for moving surfaces. *AIAA J.* 36(8):1379–86
Brentner KS, Farassat F. 2003. Modeling aerodynamically generated sound of helicopter rotors. *Prog. Aerospace Sci.* 39(2–3):83–120
Bridges J, Wernet MP. 2002. Turbulence measurements of separated flow nozzles with mixing enhancement features. *AIAA Pap. 2002-2484*
Cabot WH, Moin P. 2000. Approximate wall boundary conditions in the large-eddy simulation of high Reynolds number flow. *Flow Turb. Combust.* 63(1–4):269–91
Chu BT, Kovásznay LSG. 1958. Non-linear interactions in a viscous heat-conducting compressible gas. *J. Fluid Mech.* 3:494–514

Collis SS, Ghayour K, Heinkenschloss M. 2002. Optimal control of aeroacoustic noise generated by cylinder vortex interaction. *Int. J. Aeroacoustics* 1(2):97–114

Colonius T. 2004. Modeling artificial boundary conditions for compressible flow. *Annu. Rev. Fluid Mech.* 36:315–45

Colonius T, Freund JB. 2000. Application of Lighthill's equation to a Mach 1.92 turbulent jet. *AIAA J.* 38(2):368–70

Colonius T, Lele SK. 2004. Computational aeroacoustics: progress on nonlinear problems of sound generation. *Prog. Aerospace Sci.* 40(6):345–416

Colonius T, Lele SK, Moin P. 1997. Sound generation in a mixing layer. *J. Fluid Mech.* 330:375–409

Crighton DG. 1975. Basic principles of aerodynamic noise generation. *Prog. Aerospace Sci.* 16(1):31–96

Crighton DG. 1988. Goals for computational aeroacoustics. In *Computational Acoustics: Algorithms and Applications*, ed. D Lee, RL Sternberg, MH Schultz, pp. 3–20. Amsterdam: Elsevier-North Holland

Crighton DG. 1993. Computational aeroacoustics for low Mach number flows. In *Computational Aeroacoustics*, ed. JC Hardin, MY Hussaini, pp. 50–68. New York: Springer-Verlag. 513 pp.

Crighton DG, Dowling AP, Ffowcs Williams JE, Heckl M, Leppington FG. 1992. *Modern Methods in Analytical Acoustics*. New York: Springer-Verlag. 738 pp.

Crow SC. 1970. Aerodynamic sound emission as a singular perturbation problem. *Stud. Appl. Math.* 49(1):1–44

Curle N. 1955. The influence of solid boundaries upon aerodynamic sound. *Proc. R. Soc. London Ser. A* 231(1187):505–14

Deardorff JW. 1970. A numerical study of three-dimensional turbulent channel flow at large Reynolds numbers. *J. Fluid Mech.* 41:453–80

Doak PE. 1972. Analysis of internally generated sound in continuous materials: 2. A critical review of the conceptual adequacy and physical scope of existing theories of aerodynamic noise, with special reference to supersonic jet noise. *J. Sound Vib.* 25(2):263–335

Dowling A. 1976. Convective amplification of real simple sources. *J. Fluid Mech.* 74(3):529–46

Farassat F, Myers MK. 1988. Extension of Kirchhoff's formula to radiation from moving surfaces. *J. Sound Vib.* 123(3):451–61

Ffowcs Williams JE. 1977. Aeroacoustics. *Annu. Rev. Fluid Mech.* 9:447–68

Ffowcs Williams JE, Hall LH. 1970. Aerodynamic sound generation by turbulent flow in the vicinity of a scattering half plane. *J. Fluid Mech.* 40:657–70

Ffowcs Williams JE, Hawkings DL. 1969. Sound generation by turbulence and surfaces in arbitrary motions. *Philos. Trans. R. Soc. London Ser. A* 264(1151):321–42

Freund JB. 1997. A proposed inflow/outflow boundary condition for direct computation of aerodynamic sound. *AIAA J.* 35(4):740–42

Freund JB. 2001. Noise sources in a low-Reynolds-number turbulent jet at Mach 0.9. *J. Fluid Mech.* 438:277–305

Freund JB. 2003. Noise-source turbulence statistics and the noise from a Mach 0.9 jet. *Phys. Fluids* 15(6):1788–99

Freund JB, Colonius T. 2002. POD analysis of sound generation by a turbulent jet. *AIAA Pap. 2002-0072*
Freund JB, Fleischman TG. 2002. Ray traces through unsteady jet turbulence. *Int. J. Aeroacoustics* 1(1):83–96
Freund JB, Lele SK, Moin P. 1996. Calculation of the radiated sound field using an open Kirchhoff surface. *AIAA J.* 34(5):909–16
Freund JB, Lele SK, Moin P. 2000. Direct numerical simulation of a Mach 1.92 turbulent jet and its sound field. *AIAA J.* 38(11):2023–31
Freund JB, Samanta A, Wei M, Lele SK. 2005. The robustness of acoustic analogies. *AIAA Pap. 2005-2940*
Germano M, Piomelli U, Moin P, Cabot WH. 1991. A dynamic subgrid-scale eddy viscosity model. *Phys. Fluids A* 3(7):1760–65
Gloerfelt X, Bailly C, Juve D. 2003. Direct computation of the noise radiated by a subsonic cavity flow and application of integral methods. *J. Sound Vib.* 266(1):119–46
Goldstein ME. 1975. The low frequency sound from multipole sources in axisymmetric shear flows, with applications to jet noise. *J. Fluid Mech.* 70:595–604
Goldstein ME. 1976. *Aeroacoustics*. New York: McGraw-Hill. 293 pp.
Goldstein ME. 1984. Aeroacoustics of turbulent shear flows. *Annu. Rev. Fluid Mech.* 16:263–85
Goldstein ME. 2003. A generalized acoustic analogy. *J. Fluid Mech.* 488:315–33
Goldstein ME, Leib SJ. 2005. The role of instability waves in predicting jet noise. *J. Fluid Mech.* 525:37–72
Haj-Hariri H, Akylas TR. 1985. The wall-shear-stress contribution to boundary-layer noise. *Phys. Fluids* 28(9):2727–29
He G-W, Rubinstein R, Wang L-P. 2002. Effects of subgrid scale modeling on time correlations in large eddy simulation. *Phys. Fluids* 14(7):2186–93
He G-W, Wang M, Lele SK. 2004. On the computation of space-time correlations by large-eddy simulation. *Phys. Fluids* 16(11):3859–67
Hedges LS, Travin A, Spalart PR. 2002. Detached-eddy simulations over a simplified landing gear. *J. Fluid Eng.* 124(2):413–23
Herbert K, Leehey P, Haj-Hariri H. 1999. On the Mach- and Reynolds-number dependence of the flat-plate turbulent boundary layer wall-pressure spectrum. *Theor. Comput. Fluid Dyn.* 13(1):33–56
Howe MS. 1975. Contributions to the theory of aerodynamic sound, with application to excess jet noise and the theory of the flute. *J. Fluid Mech.* 71:625–73
Howe MS. 1979. The role of surface shear stress fluctuations in the generation of boundary layer noise. *J. Sound Vib.* 65(2):159–64
Howe MS. 1995. The damping of sound by wall turbulent shear layers. *J. Acoust. Soc. Am.* 98(3):1723–30
Howe MS. 1999. Trailing edge noise at low Mach numbers. *J. Sound Vib.* 225(2):211–38
Howe MS. 2003. *Theory of Vortex Sound*. New York: Cambridge Univ. Press. 216 pp.
Hu FQ, Hussaini MY, Manthey JL. 1996. Low-dissipation and low-dispersion Runge-Kutta schemes for computational aeroacoustics. *J. Comp. Phys.* 124(1): 177–91

Hu ZW, Morfey CL, Sandham ND. 2002. Aeroacoustics of wall-bounded turbulent flows. *AIAA J.* 40(3):465–73

Hu ZW, Morfey CL, Sandham ND. 2003. Sound radiation in turbulent channel flows. *J. Fluid Mech.* 475:269–302

Hughes TJR, Mazzei L, Oberai AA, Wray AA. 2001. The multiscale formulation of large-eddy simulation: Decay of homogeneous isotropic turbulence. *Phys. Fluids* 13(2):505–12

Inoue O, Hattori Y, Sasaki T. 2000. Sound generation by coaxial collision of two vortex rings. *J. Fluid Mech.* 424:327–65

Khavaran A, Bridges J. 2005. Modelling of fine-scale turbulence mixing noise. *J. Sound Vib.* 279(3–5):1131–54

Kurbatskii KA, Mankbadi RR. 2004. Review of computational aeroacoustics algorithms. *Int. J. Comput. Fluid Dyn.* 18(6):533–46

Landahl MT. 1975. Wave mechanics of boundary layer turbulence and noise. *J. Acoust. Soc. Am.* 57(4):824–31

Lele SK. 1992. Compact finite difference schemes with spectral-like resolution. *J. Comp. Phys.* 103(1):16–42

Lighthill MJ. 1952. On sound generated aerodynamically: I. General theory. *Proc. R. Soc. London Ser. A* 211(1107):564–87

Lilley GM. 1974. On the noise from jets. *AGARD Tech. Rep. CP-131*

Lilley GM. 1996. The radiated noise from isotropic turbulence with applications to the theory of jet noise. *J. Sound Vib.* 190(3):463–76

Lilly DK. 1992. A proposed modification of the Germano subgrid scale closure method. *Phys. Fluids A* 4(3):633–35

Lyrintzis AS. 2003. Integral acoustic methods: From the (CFD) near-field to the (acoustic) far-field. *Int. J. Aeroacoustics* 2(2):95–128

Manning TA, Lele SK. 2000. A numerical investigation of sound generation in supersonic jet screech. *AIAA/CEAS Pap. 2000-2081*

Manoha E, Troff B, Sagaut P. 2000. Trailing edge noise prediction using large eddy simulation and acoustic analogy. *AIAA J.* 38(4):575–83

Marsden AL, Wang M, Dennis JE, Moin P. 2004a. Optimal aeroacoustic shape design using the surrogate management framework. *Optim. Eng.* 5(2):235–62

Marsden AL, Wang M, Dennis JE, Moin P. 2004b. Suppression of vortex shedding noise via derivative-free shape optimization. *Phys. Fluids* 16(10):L83–86

Marsden AL, Wang M, Dennis JE, Moin P. 2005. Aerodynamic noise control by optimal shape design. *Tech. Rep. TF-96*, Dep. Mech. Eng., Stanford Univ., Stanford, CA

Mitchell BE, Lele SK, Moin P. 1992. Direct computation of the sound from a compressible co-rotating vortex pair. *AIAA Pap. 92-0374*

Mitchell BE, Lele SK, Moin P. 1995. Direct computation of the sound from a compressible co-rotating vortex pair. *J. Fluid Mech.* 285:181–202

Mohseni K, Colonius T, Freund JB. 2002. An evaluation of linear instability waves as sources of sound in a supersonic turbulent jet. *Phys. Fluids* 14(10):3593–600

Moin P. 2002. Advances in large-eddy simulation methodology for complex flows. *Int. J. Heat Fluid Flow* 23(5):710–20

Moin P, Squires KD, Cabot WH, Lee S. 1991. A dynamic subgrid-scale model for compressible turbulence and scalar transport. *Phys. Fluids A* 3(11):2746–57

Morfey CL. 2003. The role of viscosity in aerodynamic sound generation. *Int. J. Aeroacoustics* 2(3–4):225–40

Oberai AA, Roknaldin F, Hughes TJR. 2000. Computational procedures for determining structural-acoustic response due to hydrodynamic sources. *Comput. Methods Appl. Mech. Eng.* 190(3–4):345–61

Oberai AA, Roknaldin F, Hughes TJR. 2002. Computation of trailing-edge noise due to turbulent flow over an airfoil. *AIAA J.* 40(11):2206–16

Peake N, Crighton DG. 2000. Active control of sound. *Annu. Rev. Fluid Mech.* 32:137–64

Piomelli U, Balaras E. 2002. Wall-layer models for large-eddy simulations. *Annu. Rev. Fluid Mech.* 34:349–74

Piomelli U, Streett CL, Sarkar S. 1997. On the computation of sound by large-eddy simulations. *J. Eng. Math.* 32:217–36

Powell A. 1960. Aerodynamic noise and the plane boundary. *J. Acoust. Soc. Am.* 32(8):982–90

Powell A. 1964. Theory of vortex sound. *J. Acoust. Soc. Am.* 36(1):177–95

Pridmore-Brown DC. 1958. Sound propagation in a fluid flowing through an attenuating duct. *J. Fluid Mech.* 9:1–28

Ran H, Colonius T. 2004. Numerical simulation of sound radiated from a turbulent vortex ring. *AIAA Pap. 2004-2918*

Ribner HS. 1969. Quadrupole correlations governing the pattern of jet noise. *J. Fluid Mech.* 38(1):1–24

Seror C, Sagaut P, Bailly C, Juvé D. 2000. Subgrid-scale contribution to noise production in decaying isotropic turbulence. *AIAA J.* 38(10):1795–803

Seror C, Sagaut P, Bailly C, Juvé D. 2001. On the radiated noise computed by large-eddy simulation. *Phys. Fluids* 13(2):476–87

Shariff K, Wang M. 2005. A numerical experiment to determine whether surface shear-stress fluctuations are a true sound source. *Phys. Fluids*. In press

Shen H, Tam CKW. 2000. Effects of jet temperature and nozzle-lip thickness on screech tones. *AIAA J.* 38(5):762–67

Shen H, Tam CKW. 2002. Three-dimensional numerical simulation of the jet screech phenomenon. *AIAA J.* 40(1):33–41

Shur ML, Spalart PR, Strelets MKh. 2005a. Noise prediction for increasingly complex jets. Part I: methods and tests. *Int. J. Aeroacoustics.* 4:213–46

Shur ML, Spalart PR, Strelets MKh. 2005b. Noise prediction for increasingly complex jets. Part II: applications. *Int. J. Aeroacoustics.* 4:247–66

Singer BA, Brentner KS, Lockard DP, Lilley GM. 2000. Simulation of acoustic scattering from a trailing edge. *J. Sound Vib.* 230(3):541–60

Singer BA, Guo Y. 2004. Development of computational aeroacoustics tools for airframe noise calculations. *Int. J. Comput. Fluid Dyn.* 18(6):455–69

Smagorinsky J. 1963. General circulation experiments with the primitive equations. I. The basic experiment. *Mon. Weather Rev.* 91:99–164

Spalart PR, Jou WH, Strelets M, Allmaras SR. 1997. Comments on the feasibility of LES for wings and a hybrid RANS/LES approach. In *Advances in DNS/LES. Proc. 1st AFOSR Int. Conf. DNS/LES*, ed. C Liu, Z Liu, L Sakell, pp. 137–47. Columbus, OH: Greyden. 676 pp.

Stolz S, Adams NA. 1999. An approximate deconvolution procedure for large-eddy simulation. *Phys. Fluids* 11(7):1699–701

Stromberg JL, McLaughlin DK, Troutt TR. 1980. Flow field and acoustic properties of a Mach number 0.9 jet at a low Reynolds number. *J. Sound Vib.* 72(2):159–76

Suzuki T, Lele SK. 2003. Shock leakage through an unsteady vortex-laden mixing layer: application to jet screech. *J. Fluid Mech.* 490:139–67

Tam CKW. 2004. Computational aeroacoustics: an overview of computational challenges and applications. *Int. J. Comput. Fluid Dyn.* 18(6):547–67

Tam CKW, Auriault L. 1999. Jet mixing noise from fine-scale turbulence. *AIAA J.* 37(2):145–53

Tam CKW, Webb JC. 1993. Dispersion-relation-preserving finite difference schemes for computational acoustics. *J. Comp. Phys.* 107(2):262–81

Tanna HK. 1977. An experimental study of jet noise. Part I: Turbulent mixing noise. *J. Sound Vib.* 50(3):405–28

Travin A, Shur M, Strelets M, Spalart P. 2000. Detached-eddy simulations past a circular cylinder. *Flow Turb. Combust.* 63(1–4):293–313

Wang M, Freund JB, Lele SK. 2005. Computational prediction of flow generated sound. *CTR Manuscript 190*, Cent. Turbul. Res., Stanford Univ./NASA Ames, Stanford, CA

Wang M, Lele SK, Moin P. 1996a. Computation of quadrupole noise using acoustic analogy. *AIAA J.* 34(11):2247–54

Wang M, Lele SK, Moin P. 1996b. Sound radiation during local laminar breakdown in a low Mach number boundary layer. *J. Fluid Mech.* 319:197–218

Wang M, Moin P. 2000. Computation of trailing-edge flow and noise using large-eddy simulation. *AIAA J.* 38(12):2201–9

Wang M, Moin P. 2002. Dynamic wall modeling for large-eddy simulation of complex turbulent flows. *Phys. Fluids* 14(7):2043–51

Wang M, Moreau S, Iaccarino G, Roger M. 2004. LES prediction of pressure fluctuations on a low-speed airfoil. *Annu. Res. Briefs*, Cent. Turbul. Res., Stanford Univ./NASA Ames, Stanford, CA, pp. 183–93

Wei M, Freund JB. 2005. A noise-controlled free shear flow. *J. Fluid Mech.* In press

Wells VL, Renaut RA. 1997. Computing aerodynamically generated noise. *Annu. Rev. Fluid Mech.* 29:161–99

Annual Review of
Fluid Mechanics

Volume 38, 2006

Contents